

Comparison of Invariant Manifolds for Model Reduction in Chemical Kinetics

Eliodoro Chiavazzo¹, Alexander N. Gorban² and Iliya V. Karlin^{1,*}

¹ *Aerothermochemistry and Combustion Systems Laboratory LAV, ETH Zurich, 8092 Zurich, Switzerland.*

² *Department of Mathematics, University of Leicester, Leicester LE1 7RH, UK.*

Received 8 November 2006; Accepted (in revised version) 31 January 2007

Available online 30 March 2007

Abstract. A modern approach to model reduction in chemical kinetics is often based on the notion of slow invariant manifold. The goal of this paper is to give a comparison of various methods of construction of slow invariant manifolds using a simple Michaelis-Menten catalytic reaction. We explore a recently introduced Method of Invariant Grids (MIG) for iteratively solving the invariance equation. Various initial approximations for the grid are considered such as Quasi Equilibrium Manifold, Spectral Quasi Equilibrium Manifold, Intrinsic Low Dimensional Manifold and Symmetric Entropic Intrinsic Low Dimensional Manifold. Slow invariant manifold was also computed using the Computational Singular Perturbation (CSP) method. A comparison between MIG and CSP is also reported.

PACS (2006): 05.20.Dd, 82.37.-j

Key words: Chemical kinetics, model reduction, invariant manifold, entropy, nonlinear dynamics, mathematical modeling.

1 Introduction

The idea that dissipative systems of chemical kinetics can have a simplified description in terms of fast and slow motions derives from some evidences found out when such systems are integrated numerically. Indeed, a typical behavior of trajectories in the phase space during the relaxation reveals that they quickly move toward a lower dimension manifold and then, when it is reached, do not leave it anymore, proceeding slowly along it toward the equilibrium. Now it is straightforward to understand why, if such a manifold exists, it can be termed the Slow Invariant Manifold (SIM), and that it provides a simplification to the original system. Several methods were proposed to find the SIM:

*Corresponding author. *Email addresses:* chiavazzo@lav.mavt.ethz.ch (E. Chiavazzo), ag153@leicester.ac.uk (A. N. Gorban), karlin@lav.mavt.ethz.ch (I. V. Karlin)

Method of Invariant Manifolds (MIM), Method of Invariant Grids (MIG), Computational Singular Perturbation (CSP), as well as constructive approximations to SIM such as the Intrinsic Low Dimensional Manifold (ILDm). In this paper, we want to compare various methods aimed at constructing the SIM for a simple yet non-trivial test-case. In particular, we deal with three essentially different iterative algorithms:

1. *MIG-approach* (based on the Newton method) [2, 3, 5],
2. *MIG-approach* (based on the relaxation method) [2, 3, 5],
3. *CSP-approach* [11, 12].

Every iterative procedure needs an initial approximation from which it starts a refinement. In general, the quality of this initial step is important for both the convergence toward the solution and for the method efficiency; that is why different initial approximations are considered, too. For our test-case, the following approximations were used:

1. *Quasi-Equilibrium-Manifold* (QEM) [2, 3],
2. *Spectral-Quasi-Equilibrium-Manifold* (SQEM),
3. *Intrinsic-Low-Dimensional-Manifold* (ILDm) [8, 9],
4. *Symmetric-Entropic-Intrinsic-Low-Dimensional-Manifold* (SEILDm) [2, 3].

The paper is organized as follows. In Section 2, for the sake of completeness, we outline the basic notions: invariant manifold, slow manifold and invariant grid, equations of chemical kinetics and the methods of model reduction. In particular, in Section 2.2, the general equations of dissipative reaction kinetics are reviewed and cast in a form which is used throughout the paper. The *Method of Invariant Grid* (MIG) and *thermodynamic projector* concepts are discussed, providing a way to implement the MIG iteratively according to both the *Newton method with incomplete linearization* and the *relaxation method* (Section 2.1, for a general setting, and Section 2.3 for chemical kinetics). Here we also describe the *CSP method* (Section 2.4) and some possible initial approximations of SIM (Section 2.5). In Section 3, we consider a two-step four-component catalytic reaction (Michaelis-Menten mechanism) as a test case. Various initial approximations for that case are found (Sections 3.1, 3.2, 3.3). Starting from these initial approximations, MIG iterations are carried out and compared on the base of both Hausdorff norm and a measure of the invariance defect (Sections 3.4, 3.5). In Section 3.6, the CSP method is used to construct the SIM in this example, and a comparison with MIG is presented. Finally, results are discussed in Section 4.

2 Theoretical background

2.1 Slow invariant manifold (SIM)

In this section, we introduce the notions of (positively) invariant manifold, slow invariant manifold, invariant grid, and slow invariant grid, for a general system of autonomous

ordinary differential equations in a domain \mathcal{D} in \mathbf{R}^n ,

$$\dot{c} = J(c). \quad (2.1)$$

2.1.1 Invariant manifold and invariance equation

A submanifold $\Omega \subset \mathcal{D}$ is a *positively invariant manifold* for the system (2.1) if, for any solution $c(t)$, inclusion $c(t_0) \in \Omega$ implies that $c(t) \in \Omega$ for $t > t_0$. With some abuse of language, one often calls such a set Ω an invariant manifold.

For each point $c \in \Omega$, the tangent space $T_c \Omega$ is defined. If Ω is positively invariant due to system (2.1), then vector $J(c)$ belongs to this tangent space. This gives us a necessary differential condition of invariance

$$J(c) \in T_c \Omega. \quad (2.2)$$

In order to transform the inclusion condition (2.2) into an equation, we need to execute the following steps:

- to take a complement to T_c in \mathbf{R}^n , $\mathbf{R}^n = T_c \oplus E_c$,
- to split $J(c)$ into two components: $J(c) = J_{\parallel}(c) + J_{\perp}(c)$, $J_{\parallel}(c) \in T_c$, $J_{\perp}(c) \in E_c$,
- to write down an equation, $J_{\perp}(c) = 0$.

These operations are conveniently described by means of projector operators. Let for any subspace T_c a projector P on T_c be defined with image $\text{im}P = T_c$ and kernel $\text{ker}P = E_c$. Then the necessary differential condition of invariance takes the following form

$$(1 - P)J = 0. \quad (2.3)$$

The left hand side of this equation is important for many constructions and has its own name, the *defect of invariance*: $\Delta = J_{\perp} = (1 - P)J$. In this *invariance equation* (2.3) an unknown function is the manifold Ω . This manifold has to be represented in a parametric form, as an immersion $F: \mathcal{W} \rightarrow \mathcal{D}$ of a domain \mathcal{W} in the parameter space into the domain \mathcal{D} ; Ω is the image of this immersion: $\Omega = F(\mathcal{W})$.

The tangent space at the point $F(y)$ is the image of the differential of F at the point y . Hence, Eq. (2.3) is a differential equation for F . The theory of analytic solutions of this equation with analytic vector field J near an equilibrium was developed by Lyapunov [13] (the Lyapunov auxiliary theorem). Applications of this theorem to model reduction were developed recently [14].

Projector P depends on the point c and the space T_c . Invariance equations for different choice of this projector field P are equivalent, the only requirement is $\text{im}P = T_c$. But the convergence properties of computational methods significantly depend on the projector choice. The definition of slowness can also be sensitive to this choice.

At a first glance, there exists a natural method for projector field P construction: if for any c a positive definite inner product $\langle x, y \rangle_c$ (a Riemannian structure) is defined, then we can choose P as $\langle \cdot, \cdot \rangle_c$ -orthogonal projector, and $J(c) = J_{\parallel}(c) + J_{\perp}(c)$ is $\langle \cdot, \cdot \rangle_c$ -orthogonal

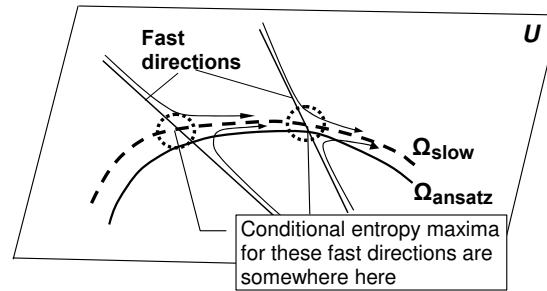


Figure 1: Fast–slow decomposition. Bold dashed line – slow invariant manifold; bold line – approximate invariant manifold; several trajectories and correspondent directions of fast motion are presented schematically.

splitting. A more careful analysis shows that this idea is “almost true”, and after some modifications leads to the *thermodynamic projector* [1, 21] (see Section 2.3.3 below). The relevant Riemannian structure is generated by the second differential of the entropy.

In a majority of applications, we are looking not for an approximation to an invariant manifold that definitely exists, but rather for an *approximate invariant manifold* with sufficiently small defect of invariance Δ ($\|\Delta\| \ll \|J\|$, for example).

2.1.2 Slow manifold

Reduction of description for dissipative kinetics assumes (explicitly or implicitly) the following picture (Fig. 1): There exists a manifold of slow motions Ω_{slow} in the space of distributions. From the initial conditions the system goes quickly in a small neighborhood of the manifold, and after that moves slowly along it. The manifold of slow motions (slow manifold, for short) must be positively invariant: if a solution starts on the manifold at t_0 , then it stays on the manifold at $t > t_0$. In some neighborhood of the slow manifold the directions of fast motion can be defined. Of course, we always do not deal with the invariant slow manifold, but with some approximate slow manifold Ω . Thermodynamics is useful for model reduction in dissipative systems. The governing idea of these applications is [1]: during the fast motion the entropy should increase, hence, the point of entropy maximum on the plane of rapid motion is not far from the slow manifold, in the area where fast and slow motion have comparable velocities (Fig. 1, inside dashed circles). This implies that *differential of the entropy at points near the slow manifold almost annihilates the planes of fast motions* (i.e. entropy gradient is almost orthogonal to these planes). For sufficiently strong fast–slow time separation the fast invariant subspace of a Jacobian near the slow manifold approximates the plane of fast motions, hence, this invariant subspace is also nearly orthogonal to the entropy gradient.

All the definitions of slow manifold for a given system are based on the comparison of motion *to* the manifold with motion *along* the manifold. There should be relatively fast contraction in selected transversal directions (in directions of projector kernel) and relatively slow change of vector field tangent component along manifold. In this paper,

we do not review all these approaches (the spectral gap condition, the cone condition, various stability conditions), the details and further references are in Refs. [16–20].

For our approach, the slow invariant manifold is the *stable fixed point* of one of the following processes:

1. Relaxation due to a film extension of dynamics [5], that is defined by the equation for immersed manifold motion with velocity $J_{\perp}(c)$:

$$\frac{dF(y)}{dt} = (1 - P)J; \quad (2.4)$$

2. Iterations of the *Newton method with incomplete linearization* for invariance equation (2.3), that is the Newton process without linearization of P : we take J in the first approximation, while for P use the zero one (for details see below and [5]).

If the Newton method with incomplete linearization converges, then it leads to slow manifold in the usual sense while the standard Newton method does not. (This is very convenient because the standard method is also much more complicated.) For sufficiently strong fast-slow time separation, most of the numerous definitions of slow invariant manifold give the same result (exactly the same, or up to higher order terms, it depends on the required regularity of manifolds).

Remark 2.1. Fast-slow motion separation in a vicinity of a wandering point[†] is not invariant with respect to smooth or analytical coordinate transformations. In vicinity of attractors (equilibria, closed orbits, or more complicated attractors) Lyapunov exponents exist, they are invariant with respect to smooth coordinate transformation. It is possible to perform invariant fast-slow separation on the base of these exponent values, and then continue the slow manifold to the areas of wandering points, in a spirit of the Lyapunov auxiliary theorem that is proved for a fixed point vicinity. For dissipative systems, most part of phase space consists of wandering points.

If we have found an approximate slow invariant manifold Ω , then the correspondent slow *reduced system* is the system on the manifold Ω defined by the projected vector field:

$$\dot{c} = PJ(c), \quad (2.5)$$

where $c \in \Omega$ and projector $P: R^n \rightarrow T_c\Omega$ depends on the point c and on the tangent space $T_c\Omega$, both.

Because F is immersion, differential $F(y)$, $DF(y)$, is reversible on its image, $T_{F(y)}\Omega$. Hence, reduced system (2.5) defines dynamics in the parameter space:

$$\dot{y} = (DF(y))^{-1}(PJ(F(y))). \quad (2.6)$$

[†] c_0 is a wandering point of system (2.1) if it has such a vicinity \mathcal{U} that for some $T > 0$ any motion $c(t)$ that starts in \mathcal{U} ($c(0) \in \mathcal{U}$) does not return in \mathcal{U} after time T ($c(t) \notin \mathcal{U}$ for $t > T$).

2.1.3 Uniqueness, stability and analyticity

Usually, there exist many solutions to invariance equation which could be considered as “slow manifolds”. For example, any semi-trajectory $\{c(t) | t > 0\}$ is positively invariant. In a vicinity of a stable fixed point, almost all solutions have the slowest Lyapunov exponent. Hence, almost all semi-trajectories could be considered as slow invariant 1D manifolds, because they meet intuitive expectations asymptotically, at $t \rightarrow \infty$. Nevertheless, it remains desirable to select a slow manifold that is the best, in some sense. As it was demonstrated in Ref. [5], definition of slow manifold as a stable point of relaxation or iteration process reduces the set of solutions, and, for example, near a typical stable fixed point of an analytical system guarantees uniqueness of analytical slow invariant manifold. For such systems, our approach gives the same analytical manifolds as the Lyapunov auxiliary theorem [13]. In this theorem, the selection principle is analyticity of manifolds near a fixed point. For a system with analytical right-hand side there exists (generically) a unique analytical invariant manifold (solution of 2.3) which is tangent to a subspace of slow solutions of linearized system. Exact statements and details could be found in Refs. [5, 13, 14, 23]. The stability based approach could be applied wider, for example, to manifolds with violation of analyticity and not only near fixed points. The well known “cone condition” and “strong squeezing property” [15–17] are, in their essence, stability conditions. The invariance of a manifold does not depend on the choice of projector P , but the stability properties could depend: this projector provides the separation of motion onto motion to the manifold (with velocity in $\ker P$) and along the manifold (with velocity in $\text{im} P$).

2.1.4 Slow invariant grids

For computational purposes, the discrete analogue of the problem of slow invariant manifold was developed in Refs. [2, 3].

We are looking for SIM as an immersion F of the parameter domain \mathcal{W} into \mathcal{D} , $F: \mathcal{W} \rightarrow \mathcal{D}$. Now we consider a discrete subset $\mathcal{G} \subset \mathcal{W}$. All functions are given on \mathcal{G} , and their smooth continuation on \mathcal{W} could be constructed by various approximation technique. We use notation $F|_{\mathcal{G}}$ for restriction a function on grid. Approximation technique gives a smooth function $F[F|_{\mathcal{G}}]$. Let the transformation of discrete set of values into a smooth function,

$$F|_{\mathcal{G}} \mapsto F[F|_{\mathcal{G}}],$$

be chosen. For each $y \in \mathcal{G}$ image of the differential $D_y F[F|_{\mathcal{G}}](y)$ is a “tangent plain” to discrete set $F|_{\mathcal{G}}$ (\mathcal{G} at point $F|_{\mathcal{G}}(y)$): $T_y = \text{im} D_y F[F|_{\mathcal{G}}](y)$. We call $F|_{\mathcal{G}}(\mathcal{G})$ an *invariant grid*, if it satisfies the grid version of invariance equation:

$$(1 - P)J(F(y)) = 0 \quad \text{for } y \in \mathcal{G}, \quad P: \mathbb{R}^n \rightarrow T_y. \quad (2.7)$$

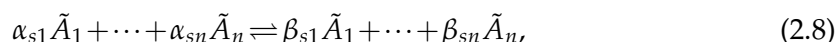
The grid version of the film equation (2.4) is also a motion in the defect of invariance direction $(1 - P)J(F(y))$, the Newton method with incomplete linearization has the same form as for continuous manifolds. Hence, we can define the *slow invariant grid* as a stable

fixed point of (one of) these processes. Formula (2.6) gives a velocity vector field on \mathcal{G} and the approximation methods continue this vector field on the parameter space \mathcal{W} . This is the reduced model.

In this paper, we shall focus our attention solely on the construction of invariant grids.

2.2 Dissipative reaction kinetics

In a closed system with n chemical species $\tilde{A}_1, \dots, \tilde{A}_n$, participating in a complex reaction, a generic reaction step can be written as a stoichiometric equation:



where s is the reaction index, $s = 1, \dots, r$ (r steps in total), and the integers α_{si} and β_{si} are stoichiometric coefficients of the step s . For each reaction step, we can introduce n -component vectors α_s and β_s , with components α_{si} and β_{si} , and the stoichiometric vector $\gamma_s = \beta_s - \alpha_s$. For every \tilde{A}_i the *extensive variable* N_i describes the number of particles of that species. If V is the volume, then the concentration of \tilde{A}_i is $c_i = N_i/V$. Dynamics of the species concentration according to the stoichiometric mechanism (2.8) reads:

$$\dot{N} = VJ(\mathbf{c}), \quad J(\mathbf{c}) = \sum_{s=1}^r \gamma_s W_s(\mathbf{c}), \quad (2.9)$$

where dot denotes the time derivative and $W_s(\mathbf{c})$ is the reaction rate function of the step s . In particular, the polynomial form of the reaction rate function is provided by *the mass action law*:

$$W_s(\mathbf{c}) = W_s^+(\mathbf{c}) - W_s^-(\mathbf{c}) = k_s^+(T) \prod_{i=1}^n c_i^{\alpha_i} - k_s^-(T) \prod_{i=1}^n c_i^{\beta_i}, \quad (2.10)$$

where $k_s^+(T)$ and $k_s^-(T)$ are the constants of the direct and of the inverse reactions rates of the step s respectively. A most popular form of their dependence is given by the Arrhenius equation:

$$k_s^\pm(T) = a_s^\pm T^{b_s^\pm} \exp(S_s^\pm/k_B) \exp(-H_s^\pm/k_B T).$$

In the latter equation, a_s^\pm, b_s^\pm are constants and H_s^\pm, S_s^\pm activation enthalpies and entropies respectively. The rate constants are not independent. Indeed, the *principle of detail balance* gives a relation between these quantities:

$$W_s^+(\mathbf{c}^{eq}) = W_s^-(\mathbf{c}^{eq}), \quad \forall s = 1, \dots, r, \quad (2.11)$$

where the positive vector $\mathbf{c}^{eq}(T)$ is the equilibrium of the system (2.9). In order to obtain a closed system of equations, one should supply an equation for the volume V . For an isolated system the extra-equations are $U, V = \text{const}$ (where U is the internal energy), for an isochoric isothermal system we get $V, T = \text{const}$, and so forth. For example, Eq. (2.9) in the latter case simply takes the form:

$$\dot{\mathbf{c}} = \sum_{s=1}^r \gamma_s W_s(\mathbf{c}) = J(\mathbf{c}). \quad (2.12)$$

Finally, also other linear constraints, related to the conservation of atoms, must be considered. In general such conservation laws can have the following form:

$$Dc = \mathbf{Const.}, \quad (2.13)$$

where l fixed and linearly independent vectors d_i are the rows of the $l \times n$ matrix D , and $\mathbf{Const.}$ is a constant vector. Equations (2.9) and (2.13), once that the thermodynamic features of the system have been defined, constitute the kind of dissipative systems which we are interested in.

2.3 Outline of the method of invariant grids

2.3.1 Thermodynamic potential

In this section, we give an outline of the MIG for chemical kinetics. For details see Refs. [1–3, 5].

If we turn our attention to perfectly stirred closed chemically active mixtures, then dissipative properties of such systems can be characterized with a thermodynamic potential which is the Lyapunov function of Eq. (2.9). That function implements Second Law of thermodynamics: it means that during the concentrations evolution in time, from the initial condition to the equilibrium state, the Lyapunov function must decrease monotonically. Therefore if $G(c)$ is the Lyapunov function, c^{eq} (equilibrium state) is its point of global minimum in the phase space. A simple example of a function G is given by the free energy of perfect gas in a constant volume and under a constant temperature:

$$G = \sum_{i=1}^n c_i [\ln(c_i / c_i^{eq}) - 1]. \quad (2.14)$$

When the function G is known, also its gradient ∇G and the second derivatives matrix $H = \|\partial^2 G / \partial c_i \partial c_j\|$ can be evaluated, so that it is possible to introduce the thermodynamic scalar product as follows:

$$\langle x, y \rangle = (x, Hy), \quad (2.15)$$

where the notation $(,)$ is the usual Euclidean scalar product.

2.3.2 The starting point: the invariance condition

Let us consider Ω as a manifold of a reduced description. The invariance requirement reads:

$$c(0) \in \Omega \Rightarrow c(t) \in \Omega, \quad \forall t \geq 0. \quad (2.16)$$

Let P be a projector on the tangent bundle of the manifold Ω . The manifold Ω is invariant with respect to the system (2.9) if and only if the following invariance equation (IE) holds:

$$[1 - P]J(c) = 0, \quad \forall c \in \Omega. \quad (2.17)$$

When the manifold is not invariant, it is not able to satisfy the invariance condition so that:

$$\exists c_0: \Delta_0 = [1 - P]J(c_0) \neq 0, \quad (2.18)$$

where Δ_0 is the defect of invariance. One way to find the SIM is to solve the IE iteratively starting from an appropriate initial manifold.

2.3.3 Thermodynamic projector

Let us now discuss further the projector appearing in the invariance equation. It is an operator which for each point $c \in \Omega$ projects the vectors $J(c)$ onto the tangent subspace of the manifold producing, in this way, the induced vector field $PJ(c)$. In general, condition (2.17) does not require any special constraint for the projector P (see Section 2.1.1). However, the thermodynamic properties of the kinetic equations (2.9) define the projector unambiguously [5]. To this end, let us define a differential of G , that is linear functional:

$$DG(x) = (\nabla G(c), x). \quad (2.19)$$

A special class of projectors is the thermodynamic one. If a projector belongs to this class then the induced vector field respects the dissipation inequality:

$$DG(PJ) \leq 0, \quad \forall c \in \Omega. \quad (2.20)$$

It has been shown that a projector P respects the (2.20) if and only if [1]:

$$\ker P \subseteq \ker DG, \quad \forall c \in \Omega, \quad (2.21)$$

where \ker denotes the null space of an operator. It is clear now that if one wants to solve Eq. (2.17), then a projector must be specified. Here we remind the way to construct the thermodynamic projector which will be used in MIG procedure. This projector depends on the concentration point c and on the tangent space to the manifold Ω .

We are looking for a grid approximation of a q -dimensional SIM. Let \mathcal{G} be a discrete subset of q dimensional parameter space \mathbf{R}^q and let $F|_{\mathcal{G}}$ be a mapping of \mathcal{G} into the concentration space. If we select an approximation procedure to restore the smooth map F from the discrete map $F|_{\mathcal{G}}$ (we need a very small part of F , derivatives of F in the grid points only), then the derivatives $f_i = \partial F / \partial y_i$ are available, and for each grid point the tangent space is:

$$T_y = \text{Lin}\{f_i\}, \quad i = 1, \dots, n. \quad (2.22)$$

We assume that one of points $y \in \mathcal{G}$ maps into equilibrium, and at other points intersection of manifold with G levels is transversal (i.e. $(DG)_{F(y)}(x) \neq 0$ for some $x \in T_y$). Let us consider the subspace $T_{0y} = (T_y \cap \ker DG)$. In order to define the thermodynamic projector, it is required, if $T_{0y} \neq T_y$, to introduce the vector e_y which satisfies the following conditions:

$$\begin{cases} e_y \in T_y, \\ \langle e_y, x \rangle = 0, \quad \forall x \in T_{0y}, \\ DG(e_y) = 1. \end{cases}$$

Let \mathbf{P}_0 be the orthogonal projector on T_{0y} with respect to the entropic scalar product (2.15), then the thermodynamic projection of vector \mathbf{x} is defined as:

$$\begin{cases} T_{0y} \neq T_y \Rightarrow \mathbf{P}\mathbf{x} = \mathbf{P}_0\mathbf{x} + \mathbf{e}_y DG(\mathbf{x}), \\ T_{0y} = T_y \Rightarrow \mathbf{P}\mathbf{x} = \mathbf{P}_0\mathbf{x}. \end{cases} \quad (2.23)$$

2.3.4 Iterative procedures: the Newton method with incomplete linearization

When MIG method is applied, not a manifold is searched as a solution, but a set of concentration points whose defect of invariance is sufficiently small: let Ω denote that solution (invariant grid). MIG is an iterative procedure: this means that, at the beginning, only an initial approximation Ω_0 of Ω is available. In general, Ω_0 does not respect the invariance condition (2.17) satisfactorily so the (2.18) holds: for this reason the position of $\mathbf{c}_0 \in \Omega_0$ must be changed. We can think to correct its position and get a new point $(\mathbf{c}_0 + \delta\mathbf{c})$ with a lower defect of invariance $\Delta = [1 - \mathbf{P}]\mathbf{J}(\mathbf{c}_0 + \delta\mathbf{c})$. If the initial node is "not far" from the invariant manifold, a reasonable way to get the node correction $\delta\mathbf{c}$ is to solve the linearized invariance equation where the vector field \mathbf{J} is expanded to the first order and the projector \mathbf{P} to the zeroth order:

$$[1 - \mathbf{P}(\mathbf{c})][\mathbf{J}(\mathbf{c}) + \mathbf{L}(\mathbf{c})\delta\mathbf{c}] = 0. \quad (2.24)$$

\mathbf{L} is the matrix of first derivatives of \mathbf{J} (Jacobian matrix). The Newton method with incomplete linearization consists of Eq. (2.24) supplied by the extra condition [1]:

$$\mathbf{P}\delta\mathbf{c} = 0. \quad (2.25)$$

The additional condition (2.25) and the atoms balances (2.13) automatically can be taken into account choosing a basis $\{\mathbf{b}_i\}$ in the subspace $\mathbf{S} = (\ker\mathbf{P} \cap \ker\mathbf{D})$. Let $h = \dim(\mathbf{S})$, then the correction can be cast in the form $\delta\mathbf{c} = \sum_{i=1}^h \delta_i \mathbf{b}_i$, so that the linearized invariance equation (2.24) becomes the linear algebraic system in terms of δ_i :

$$\sum_{i=1}^h \delta_i \langle (1 - \mathbf{P})\mathbf{L}\mathbf{b}_i, \mathbf{b}_k \rangle = - \langle (1 - \mathbf{P})\mathbf{J}, \mathbf{b}_k \rangle, \quad k = 1, \dots, h. \quad (2.26)$$

Remark 2.2. Here the usual scalar product $\langle \cdot, \cdot \rangle$ was used to get the components of the left-hand side of (2.24) in the basis vectors $\{\mathbf{b}_i\}$. Nevertheless, a different scalar product can be also used without losing generality.

In the case of the thermodynamic projector, it proves convenient to choose the basis $\{\mathbf{b}_i\}$ orthonormal with respect to the entropic scalar product (2.15) and write the (2.26) as:

$$\sum_{i=1}^h \delta_i \langle (1 - \mathbf{P})\mathbf{L}\mathbf{b}_i, \mathbf{b}_k \rangle = - \langle (1 - \mathbf{P})\mathbf{J}, \mathbf{b}_k \rangle, \quad k = 1, \dots, h. \quad (2.27)$$

The projector (2.23) is "almost" $\langle \cdot, \cdot \rangle$ -orthogonal ($\langle \text{im}\mathbf{P}, \ker\mathbf{P} \rangle \cong 0$) close to the SIM (see Section 2.1.1). Because of that special feature, Eq. (2.27) can be approximated and simplified as follows:

$$\sum_{i=1}^h \delta_i \langle \mathbf{L}\mathbf{b}_i, \mathbf{b}_k \rangle = - \langle \mathbf{J}, \mathbf{b}_k \rangle, \quad k = 1, \dots, h. \quad (2.28)$$

Note that, in general, a refinement carried out by Eq. (2.28) leaves a residual defect (2.18) in the grid nodes which cannot be annihilated although the refinement procedure continues. Therefore, when a higher accuracy in the SIM description is required, Eq. (2.26) is recommended.

2.3.5 Iterative procedures: the relaxation method

An alternative approach to solve Eq. (2.24) is the *relaxation method*. According to that method the correction is written as $c = c_0 + \tau(c)\Delta(c)$, and the quantity $\tau(c)$ is obtained from the condition:

$$\langle \Delta, [1 - P][J + \tau(c)L\Delta] \rangle = 0,$$

and solving with respect to τ :

$$\tau(c) = -\frac{\langle \Delta, \Delta \rangle}{\langle \Delta, L\Delta \rangle}. \quad (2.29)$$

Eq. (2.29) shows straightforwardly that the relaxation method is explicit, but as it adjusts the node position acting only along the direction of the defect Δ , typically we expect it to be less efficient in comparison with the Newton method. On the other hand, this method is particularly easy to implement.

2.3.6 Discussion of the method of invariant grids

The invariant grid is not just a discrete approximation of the invariant manifold, but a self-standing object which can be introduced independently of that manifold. It appears to be a convenient way to represent an invariant manifold [3, 5], because, during the method implementation, only a set of concentration vectors needs to be stored instead of dealing with some complicated analytic expressions. Moreover, the Grid is a very flexible object which can be extended (by adding some more nodes, see e.g. the growing lump and invariant flags strategies [3]), contracted and refined. The method of invariant grids does not require any global parametrization, since the thermodynamic projector P in the equations (2.26-2.27) is locally constructed. The problem of the grid correction is fully decomposed into the problems of the grid's node correction. The latter feature and the locality of the projector P make MIG particularly suitable for parallel realizations.

On the other hand, as it was first pointed out in Ref. [3, 4], when one reduces the grid spacing in order to refine the grid, then, once the grid spacing becomes small enough, one can face the problem of the Courant instability [7]. Instead of converging, at every iteration the grid becomes more and more entangled. This situation is illustrated in Fig. 2a. A way to avoid such instability is well known. This is decreasing the time step. In our problem, instead of a true time step, we have a shift in the Newtonian direction. Formally, we can assign the value $\tilde{h} = 1$ for one complete step in the Newtonian direction. Let us extend now the Newton method to arbitrary \tilde{h} . For this, let us find δ_i from (2.26), but update δc proportionally to \tilde{h} ; the new value of c_{n+1} is equal to

$$c_{n+1} = c_n + \tilde{h}_n \delta c_n, \quad (2.30)$$

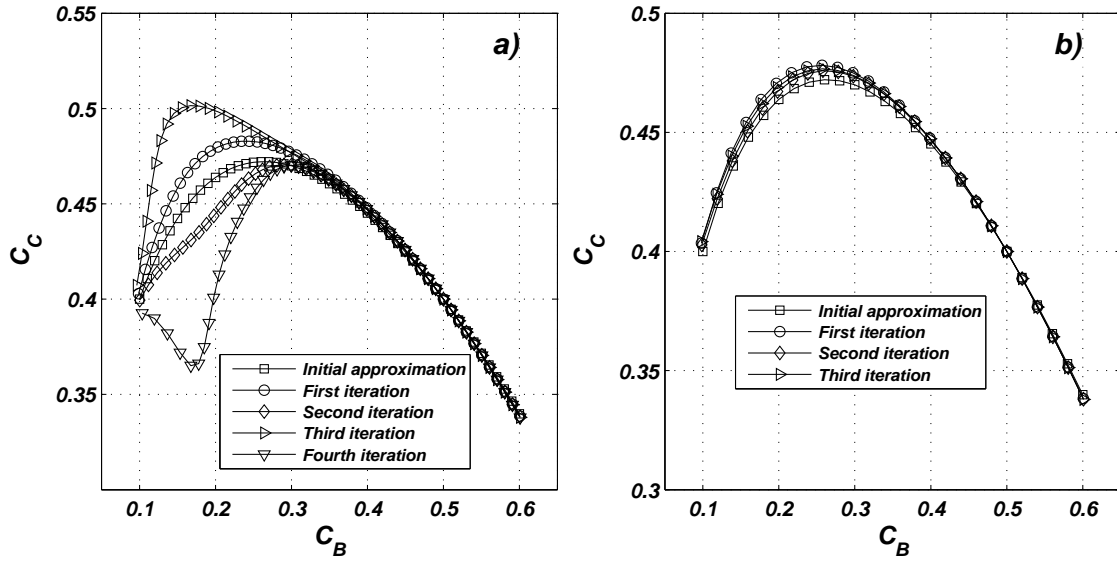


Figure 2: Invariant grid construction for a three-species, four-steps mechanism: $A \leftrightarrow B, B \leftrightarrow C, C \leftrightarrow A, A + B \leftrightarrow 2C$, with $k_1^+ = k_2^+ = k_3^+ = 1, k_4^+ = 50, C_A^{eq} = 0.1, C_B^{eq} = 0.5, C_C^{eq} = 0.4$. C_B was chosen as a reduced variable. a) In the range $C_B = [0.1, 0.6]$, the grid spacing on the initial approximation was uniformly chosen ($\Delta C_B = 0.01$) and $\tilde{h} = 1$. Newton iterations diverge. b) Grid spacing ΔC_B was increased to 0.02 and stability was recovered.

where n denotes the number of iteration. One way to choose the step value \tilde{h} is to make it adaptive, by controlling the average of the invariance defect $\|\Delta\|$ at every step. Another way is the convergence control: then $\sum \tilde{h}_n$ plays a role of time. Elimination of the Courant instability for the relaxation method can be done quite analogously. Everywhere the step \tilde{h} is maintained as large as it is possible without running into convergence problems. Finally, the rate of convergence of the invariant grid iterative construction will be accessed below through considering examples (see Section 3.5 and Fig. 8).

2.4 Outline of the computational singular perturbation algorithm

The *Computational Singular Perturbation* (CSP) method [11, 12] looks for a decomposition into fast and slow modes of the right-hand side of the system (2.12). If $a_i^f, i = 1, \dots, (n - q)$ are fast and $a_i^s, i = 1, \dots, q$ slow directions (assumed linearly independent), and if the dual basis b^i is fixed by the orthogonality relations,

$$b^i a_j = \delta_j^i, \quad i, j = 1, \dots, n, \tag{2.31}$$

where δ_j^i is Kronecker's delta, then the vector field of the n -dimensional system (2.12) is written as

$$J = A_f(B^f J) + A_s(B^s J). \tag{2.32}$$

A_f, A_s are $n \times (n-q)$ and $n \times q$ column matrices respectively formed by the fast and slow a_i vectors, while B^f, B^s are $(n-q) \times n$ and $q \times n$ matrices formed by b^i vectors. Two refinement algorithms are utilized [11, 12]. The first one regards B^f :

$$\begin{aligned} B^f(k_1+1, m_1) &= \tau(k_1, m_1) [B^f(k_1, m_1)L + \dot{B}^f(k_1, m_1)], \\ A_f(k_1+1, m_1) &= A_f(k_1, m_1), \\ B^s(k_1+1, m_1) &= B^s(k_1, m_1), \\ A_s(k_1+1, m_1) &= [I - A_f(k_1+1, m_1)B^f(k_1+1, m_1)]A_s(k_1, m_1), \end{aligned} \quad (2.33)$$

while the second one is an A_f -refinement:

$$\begin{aligned} B^f(k_2, m_2+1) &= B^f(k_2, m_2), \\ A_f(k_2, m_2+1) &= [LA_f(k_2, m_2) - \dot{A}_f(k_2, m_2)]\tau(k_2, m_2), \\ B^s(k_2, m_2+1) &= B^s(k_2, m_2)[I - A_f(k_2, m_2+1)B^f(k_2, m_2+1)], \\ A_s(k_2, m_2+1) &= A_s(k_2, m_2), \end{aligned} \quad (2.34)$$

where

$$\begin{aligned} \tau(k_i, m_i) &= \{ [B^f(k_i, m_i)L + \dot{B}^f(k_i, m_i)]A_f(k_i, m_i) \}^{-1}, \\ \dot{B}^f(k_1, m_1) &= \sum_{i=1}^n \frac{\partial B^f(k_1, m_1)}{\partial c_i} J_i, \\ \dot{A}_f(k_2, m_2) &= \sum_{i=1}^n \frac{\partial A_f(k_2, m_2)}{\partial c_i} J_i. \end{aligned}$$

Here L and $J = \{J_i\}$ denote again the Jacobian matrix and the vector field of the system (2.12).

After a sufficient number of CSP refinements, the approximate SIM equations and the simplified system are written

$$B^f J = 0, \quad (2.35)$$

$$\dot{c} = A_s(B^s J). \quad (2.36)$$

The two refinement procedures described above are defined *independent* because each index (k or m) can be increased independently. In particular, iterations on k aim to improve the accuracy in the description of the SIM, while it is expected that the other ones makes the simplified system (2.36) less and less stiff (cf. Refs. [10–12]). The orthogonality of the CSP vectors (2.31) always holds. In this paper, we are solely interest in the convergence of (2.35) to the SIM, and do not address the dynamics of the reduced system.

2.5 Initial approximation

2.5.1 Quasi equilibrium manifold

Eq. (2.13) define the polytope Q of all concentration vectors which satisfy the balance constraints. On Q , we can choose the points which minimize the Lyapunov function G of the system that we are dealing with: such a manifold is called *Quasi-Equilibrium-Manifold* (QEM). It attempts to do a motions decomposition in fast - toward the QEM - and slow - along the QEM - inasmuch as G must decrease during the fast motions. In order to be more specific, let us consider a system of n species, it has $(n-1)$ degrees of freedom because of the (2.13). If $q < (n-1)$ is the dimension of the QEM, then the variables of reduced description are $\tilde{\zeta}_1, \dots, \tilde{\zeta}_q$ so that:

$$(\mathbf{m}_1, \mathbf{c}) = \tilde{\zeta}_1, \dots, (\mathbf{m}_q, \mathbf{c}) = \tilde{\zeta}_q, \quad (2.37)$$

where \mathbf{m}_i is an n -dimensional vector. The solution of the variational problem $G \mapsto \min$, under constraints (2.13) and (2.37), represents the QEM.

2.5.2 Spectral quasi equilibrium manifold

Different QE-manifolds can be obtained choosing different sets of vectors $\{\mathbf{m}_i\}$. On the other hand, QEM is constructed just on the base of G and mass balance constraints: therefore considering the eigenvectors of Jacobian L could be a way to take into account some information about the vector field J . In order to do that, let us discuss further the Jacobian matrix calculated at the equilibrium point $L(\mathbf{c}^{eq})$. In general L can be regarded as the sum of L' and L'' , where the first matrix L' is symmetric with respect to the entropic scalar product (2.15), but it also respects the following equality: $L'(\mathbf{c}^{eq}) = L(\mathbf{c}^{eq})$ [3]. So if we take q left eigenvectors of $L(\mathbf{c}^{eq})$, which correspond to the q smallest absolute eigenvalues (slowest motions), then we construct that particular QEM called *Spectral-Quasi-Equilibrium-Manifold* (SQEM). Same result is obtained by taking $\mathbf{m}_i = H\mathbf{x}_i$, where \mathbf{x}_i is one of the q slowest right eigenvector of $L(\mathbf{c}^{eq})$, while H is the matrix of second derivatives of the Lyapunov function G at equilibrium. Indeed, if we let $\mathbf{y} = H\mathbf{x}$ be a left eigenvector of $L'(\mathbf{c}^{eq})$, then

$$L'^T(\mathbf{c}^{eq})H\mathbf{x} = \lambda H\mathbf{x},$$

where the superscript T denotes the usual transposition. So \mathbf{x} must be a right eigenvector of matrix $H^{-1}L'^T(\mathbf{c}^{eq})H = L(\mathbf{c}^{eq})$.

2.5.3 Intrinsic low dimensional manifold (ILDm)

The way to construct the ILDM (Maas & Pope et al. [8]- [9]) is based on the following separation of eigenvalues of Jacobi matrix L :

$$\max\{\text{Re}[\lambda_i], i = 1, \dots, (n-q)\} \ll \eta < \min\{\text{Re}[\lambda_i], i = (n-q+1), \dots, n\}, \quad (2.38)$$

$$\eta < 0.$$

In that way it is possible to know, in each point, the fast subspace E_C (spanned by eigenvectors which correspond to the first eigenvalues set of (2.38)), and the slow one T_C . Let us define the *transition matrix* Q as a column vectors matrix:

$$Q = (v_1, \dots, v_{n-q}, v_{n-q+1}, \dots, v_n), \quad (2.39)$$

where v_1, \dots, v_{n-q} are the fast eigenvectors of L , while v_{n-q+1}, \dots, v_n the slow ones. If we consider the inverse matrix Q^{-1} as a row vectors matrix:

$$Q^{-1} = \begin{pmatrix} \tilde{v}_1 \\ \dots \\ \tilde{v}_{n-q} \\ \tilde{v}_{n-q+1} \\ \dots \\ \tilde{v}_n \end{pmatrix} = \begin{pmatrix} \tilde{Q}_f \\ \tilde{Q}_s \end{pmatrix}, \quad (2.40)$$

with \tilde{Q}_f collecting the first $n-q$ rows of Q^{-1} , then the equation of ILDM reads:

$$\tilde{Q}_f J = 0. \quad (2.41)$$

It is important to note that operator \tilde{Q}_f is nothing but a spectral projector which can be constructed efficiently using, e.g. Schur decomposition [8,9]. In the illustrative examples below we shall not use this, because all eigenvectors will be evaluated explicitly. It is also worth to compare equations (2.35) and (2.41) and to note that they are very similar. The ILDM projector \tilde{Q}_f can be considered an approximation for the CSP-projector B^f . In that case B^f is a matrix whose rows are the fast left eigenvectors of Jacobian L .

2.5.4 Symmetric entropic intrinsic low dimensional manifold (SEILDM)

From the geometrical standpoint, the ILDM approach attempts to provide fast and slow directions approximation on the base of information of Jacobian matrix L eigenvectors. This becomes computationally intensive in large dimensions. In order to obtain a considerable simplification, it was suggested [2] to use the spectral decomposition of the symmetrized part of L , rather than L itself:

$$L^{sym} = \frac{1}{2}(L + H^{-1}L^T H), \quad (2.42)$$

where L^T denotes the usual transposed matrix. By definition L^{sym} results symmetric with respect to the entropic scalar product (2.15): the ILDM constructed considering it, instead of L , is termed *Symmetric Entropic Intrinsic Low Dimensional Manifold*. It is well known that spectral decomposition is much more viable for symmetric operators.

3 MIG and CSP method at work: a simple example

In the following, a constant volume and pressure system with three components \tilde{A}_1 , \tilde{A}_3 , \tilde{A}_4 and one catalyst \tilde{A}_2 will be taken as a test-case. Let us consider the two-step reaction:



so that function (2.14) can be utilized as the global potential, while (2.12) is the form of the kinetic equation for the four-component vector of concentrations $c = (c_1, c_2, c_3, c_4)^T$, in particular we have:

$$\dot{c} = J(c) = \gamma_1 W_1 + \gamma_2 W_2. \quad (3.3)$$

Here subscripts 1,2 denote the steps (3.1) and (3.2). Therefore stoichiometric vectors and W_s functions read:

$$\begin{aligned} \gamma_1 &= (-1, -1, 1, 0), & W_1 &= W_1^+ - W_1^- = k_1^+ c_1 c_2 - k_1^- c_3, \\ \gamma_2 &= (0, 1, -1, 1), & W_2 &= W_2^+ - W_2^- = k_2^+ c_3 - k_2^- c_2 c_4. \end{aligned} \quad (3.4)$$

The system (3.3) has a 2×4 conservation law matrix D (see Eq. (2.13)):

$$Dc = \mathbf{Const.} \Rightarrow \begin{bmatrix} 1 & 0 & 1 & 1 \\ 0 & 1 & 1 & 0 \end{bmatrix} \begin{bmatrix} c_1 \\ c_2 \\ c_3 \\ c_4 \end{bmatrix} = \begin{bmatrix} \text{const}_1 \\ \text{const}_2 \end{bmatrix}. \quad (3.5)$$

Thus, the dimension of the phase space is two and we aim at attaining an one-dimensional reduced description. A more extended notation of (3.3) is:

$$\begin{bmatrix} \dot{c}_1 \\ \dot{c}_2 \\ \dot{c}_3 \\ \dot{c}_4 \end{bmatrix} = \begin{bmatrix} J_1 \\ J_2 \\ J_3 \\ J_4 \end{bmatrix} = \begin{bmatrix} k_1^- c_3 - k_1^+ c_1 c_2 \\ k_1^- c_3 - k_1^+ c_1 c_2 + k_2^+ c_3 - k_2^- c_2 c_4 \\ k_1^+ c_1 c_2 - k_1^- c_3 + k_2^- c_2 c_4 - k_2^+ c_3 \\ k_2^+ c_3 - k_2^- c_2 c_4 \end{bmatrix}, \quad (3.6)$$

so in that case the Jacobian matrix takes the form:

$$L = \left\{ \frac{\partial J_i}{\partial c_j} \right\} = \begin{bmatrix} -k_1^+ c_2 & -k_1^+ c_1 & k_1^- & 0 \\ -k_1^+ c_2 & -k_1^+ c_1 - k_2^- c_4 & k_1^- + k_2^+ & -k_2^- c_2 \\ k_1^+ c_2 & k_1^+ c_1 + k_2^- c_4 & -k_1^- - k_2^+ & k_2^- c_2 \\ 0 & -k_2^- c_4 & k_2^+ & -k_2^- c_2 \end{bmatrix}, \quad (3.7)$$

while the gradient and second derivatives matrix of Lyapunov function G can be written as:

$$\nabla G = \begin{bmatrix} \ln c_1 - \ln c_1^{eq} \\ \ln c_2 - \ln c_2^{eq} \\ \ln c_3 - \ln c_3^{eq} \\ \ln c_4 - \ln c_4^{eq} \end{bmatrix}, \quad H = \begin{bmatrix} 1/c_1 & 0 & 0 & 0 \\ 0 & 1/c_2 & 0 & 0 \\ 0 & 0 & 1/c_3 & 0 \\ 0 & 0 & 0 & 1/c_4 \end{bmatrix}. \quad (3.8)$$

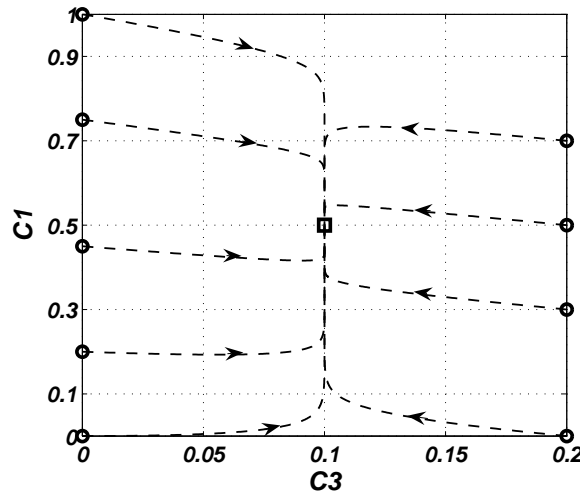


Figure 3: Solutions trajectories with different initial conditions (circles) in $c_1 - c_3$ plane. The square denotes the equilibrium point.

For our calculations the following set of parameters will be used:

$$\begin{aligned}
 k_1^+ &= 1, & k_1^- &= 0.5, & k_2^+ &= 0.4, & k_2^- &= 1, \\
 c_1^{eq} &= 0.5, & c_2^{eq} &= 0.1, & c_3^{eq} &= 0.1, & c_4^{eq} &= 0.4, \\
 const_1 &= 1, & const_2 &= 0.2.
 \end{aligned}$$

After that choice, the direct numerical integration of the system (3.3) supplies the solution trajectories shown in Fig. 3. Now it is straightforward to find out that the SIM projection onto $c_1 - c_3$ plane simply results in the line segment $c_3 = c_3^{eq} = 0.1$. So we expect that, in this example, methods of reduced description provide this manifold.

3.1 QEM on the example

In order to extract the invariant manifold of Fig. 3, we can think to construct an initial manifold, with no special effort, and then to refine it thanks to MIG procedure: that is the case when QEM is taken as first approximation. In our example $q = 1$ (one-dimensional reduced description, see Section 2.5.1). Thus, we need a 4-dimensional vector \mathbf{m} which gives the reduced description variable ζ . It is chosen $\mathbf{m} = (1, 0, 0, 0)$, so that the QEM must respect the following conditions:

$$\begin{cases}
 G = \sum_{i=1}^4 c_i [\ln(c_i/c_i^{eq}) - 1] \rightarrow \min \\
 (\mathbf{m}, \mathbf{c}) = \zeta \\
 D\mathbf{c} = (const_1, const_2)^T.
 \end{cases} \tag{3.9}$$

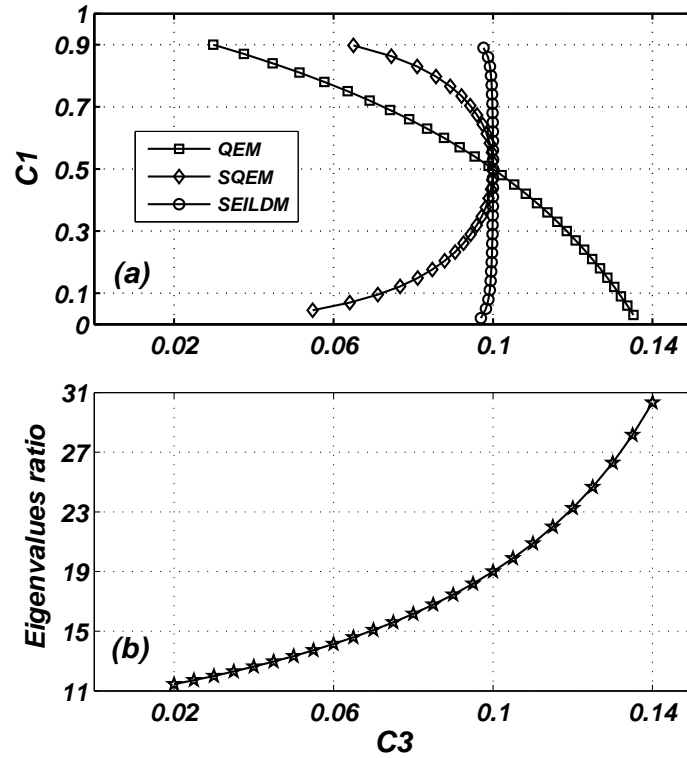


Figure 4: (a) QEM, SQEM and SEILD as initial approximations of SIM for the system (3.3). (b) Ratio between the second smallest and the smallest by absolute value nonzero eigenvalue of the Jacobian: in that case λ^f/λ^s depends only on c_3 (see (3.15)).

Note that the macroscopic parameter ζ in this example is the concentration of the component \tilde{A}_1 ($\zeta = c_1$). Let c_0 be the solution of the problem (3.9), and let ϕ be the relation between c_3 and c_1 on the QE-manifold, so that $c_{03} = \phi(\zeta)$. The problem (3.9) takes the following more explicit form:

$$\begin{cases} c_{01} = \zeta, c_{02} = const_2 - \phi(\zeta) \\ c_{03} = \phi(\zeta), c_{04} = const_1 - \zeta - \phi(\zeta) \\ \frac{\partial G(\phi, \zeta)}{\partial \phi} = 0, \frac{\partial^2 G(\phi, \zeta)}{\partial \phi^2} > 0. \end{cases} \quad (3.10)$$

The solution of the system (3.10) delivers a quadratic expression for $\phi(\zeta)$:

$$\phi(\zeta) = \Psi(\zeta) - \sqrt{\Psi^2(\zeta) - const_2(const_1 - \zeta)},$$

where $\Psi(\zeta) = (const_2(const_1 - c_1^{eq}) + c_3^{eq}(c_1^{eq} + c_3^{eq} - \zeta)) / (2c_3^{eq})$ (see Fig. 4(a)). That manifold results "quite far" from the invariant one, so the QEM decomposition of fast and slow motions cannot be considered good, and must be corrected by MIG procedure.

3.2 SQEM on the example

We can attempt to have a better accordance between the initial approximation and the SIM at least in a neighborhood of the equilibrium point. That is what the SQEM aims at when m is taken, not blindly, but choosing the slowest left eigenvector x_l^s of matrix (3.7) calculated in c^{eq} . In the following, subscripts l and r and superscripts f and s will denote left, right, fast and slow eigenvectors, respectively. Spectral analysis of the Jacobian (3.7) in the equilibrium state provides two non-zero eigenvalues:

$$\begin{aligned} \lambda^f &= -1.9, & x_l^f &= (1, 9, -9, 1), \\ \lambda^s &= -0.1, & x_l^s &= (1, 0, 0, -1.25). \end{aligned}$$

This time the choice of the reduced description variable is unambiguous ($m = x_l^s \Rightarrow \zeta = c_1 - 1.25c_4$), so the problem (3.9) becomes:

$$\begin{cases} c_{01} = 1.25\phi(\zeta) + \zeta \\ c_{02} = const_2 - const_1 + \zeta + 2.25\phi(\zeta) \\ c_{03} = const_1 - \zeta - 2.25\phi(\zeta) \\ c_{04} = \phi(\zeta) \\ \frac{\partial G(\phi, \zeta)}{\partial \phi} = 0, \frac{\partial^2 G(\phi, \zeta)}{\partial^2 \phi} > 0, \end{cases} \quad (3.11)$$

and the relation between ϕ and ζ on the SQE-manifold reads:

$$\left(\frac{\zeta + 1.25\phi}{c_1^{eq}} \right)^{1.25} \left(\frac{c_3^{eq} \zeta + 2.25\phi - 0.8}{c_2^{eq} - \zeta - 2.25\phi + 1} \right)^{2.25} \frac{\phi}{c_4^{eq}} - 1 = 0. \quad (3.12)$$

As expected, the SQEM provides a much better SIM approximation close to the equilibrium point (see Fig. 4(a)).

3.3 ILDM and SEILDM

An easier way to study the system (3.6) is to reduce the dimension from four to two by adding the two conservation laws (3.5). The ODE system of c_3 and c_1 time evolution becomes:

$$\begin{cases} \dot{c}_3 = c_3^2 - 2.1c_3 + 0.2 \\ \dot{c}_1 = 0.5c_3 + c_1c_3 - 0.2c_1. \end{cases} \quad (3.13)$$

Here the Jacobian matrix takes the simple form:

$$L(c_3, c_1) = \begin{bmatrix} 2c_3 - 2.1 & 0 \\ 0.5 + c_1 & c_3 - 0.2 \end{bmatrix}, \quad (3.14)$$

so the spectral analysis of that operator gives the following eigenvalues:

$$\lambda^f = 2c_3 - 2.1, \quad \lambda^s = c_3 - 0.2. \quad (3.15)$$

Their ratio, which can be regarded as an estimation of time scales separation, is reported in Fig. 4(b) for the domain of the phase space of interest. The right and left eigenvectors are:

$$\mathbf{x}_r^f = (c_3 - 1.9, 0.5 + c_1)^T, \quad \mathbf{x}_r^s = (0, 1)^T, \tag{3.16}$$

$$\mathbf{x}_l^f = (1, 0), \quad \mathbf{x}_l^s = (0.5 + c_1, 1.9 - c_3). \tag{3.17}$$

According to the procedure described in Section 2.5.3, being $(n - q) = 1$, $v_1 = \mathbf{x}_r^f$ and $v_2 = \mathbf{x}_r^s$, we obtain:

$$\mathbf{Q} = \begin{bmatrix} c_3 - 1.9 & 0 \\ 0.5 + c_1 & 1 \end{bmatrix} \Rightarrow \mathbf{Q}^{-1} = \frac{1}{c_3 - 1.9} \begin{bmatrix} 1 & 0 \\ -0.5 - c_1 & c_3 - 1.9 \end{bmatrix} \tag{3.18}$$

and one of the solutions of ILDM equation (2.41) for that case ($c_3^2 - 2.1c_3 + 0.2 = 0$) meets exactly the SIM.

Let us consider here the symmetrized part L^{sym} of Jacobian (3.7) calculated according to (2.42):

$$L^{sym} = 0.5 \begin{bmatrix} -2k_1^+ c_2 & -2k_1^+ c_1 & \left(k_1^- + \frac{k_1^+ c_1 c_2}{c_3}\right) & 0 \\ -2k_1^+ c_2 & -2k_1^+ c_1 - 2k_2^- c_4 & \left(k_1^- + \frac{(k_1^+ c_1 + k_2^- c_4)c_2}{c_3} + k_2^+\right) & -2k_2^- c_2 \\ \left(\frac{k_1^- c_3}{c_1} + k_1^+ c_2\right) & \left(k_1^+ c_1 + k_2^- c_4 + \frac{(k_1^- + k_2^+)c_3}{c_2}\right) & -2k_1^- - 2k_2^+ & \left(k_2^- c_2 + \frac{k_2^+ c_3}{c_4}\right) \\ 0 & -2k_2^- c_4 & \left(\frac{k_2^- c_2 c_4}{c_3} + k_2^+\right) & -2k_2^- c_2 \end{bmatrix}.$$

Note that L^{sym} is symmetric with respect to the entropic scalar product (2.15). The ILDM procedure, carried out with L^{sym} instead of L , delivers the SEILDM approximation. The 1D-grid in Fig. 4(a) was found by solving Eq. (2.41), node by node, as described in the following. Let c_j and $\zeta(j)$ be a generic node of the SEILDM grid and its correspondent reduced description variable (in our case $\zeta = c_1$), respectively. Eq. (2.41) takes the form:

$$\mathbf{x}_l^f \mathbf{J} = 0, \tag{3.19}$$

where \mathbf{x}_l^f is the fastest left eigenvector of $L^{sym}(c_j)$. Once the discretization step on the grid ($\Delta\zeta$) is defined, the grid node $c_{j\pm 1}$ can be evaluated by solving Eq. (3.19) and imposing that the macroscopic parameter $\zeta(j\pm 1) = \zeta(j) \pm \Delta\zeta$. That algorithm, starting from the equilibrium point ($c_1 = c^{eq}$), was performed twice choosing $\Delta\zeta = 0.03$: the first time to compute the upper branch of the SEILDM grid, the second time to get the other one.

3.4 MIG iterations

Let us write the thermodynamic projector (2.23) for the case (3.6). Here the tangent subspace T_y is a line spanned by the vector e_y . If f is a vector parallel to T_y and $z =$

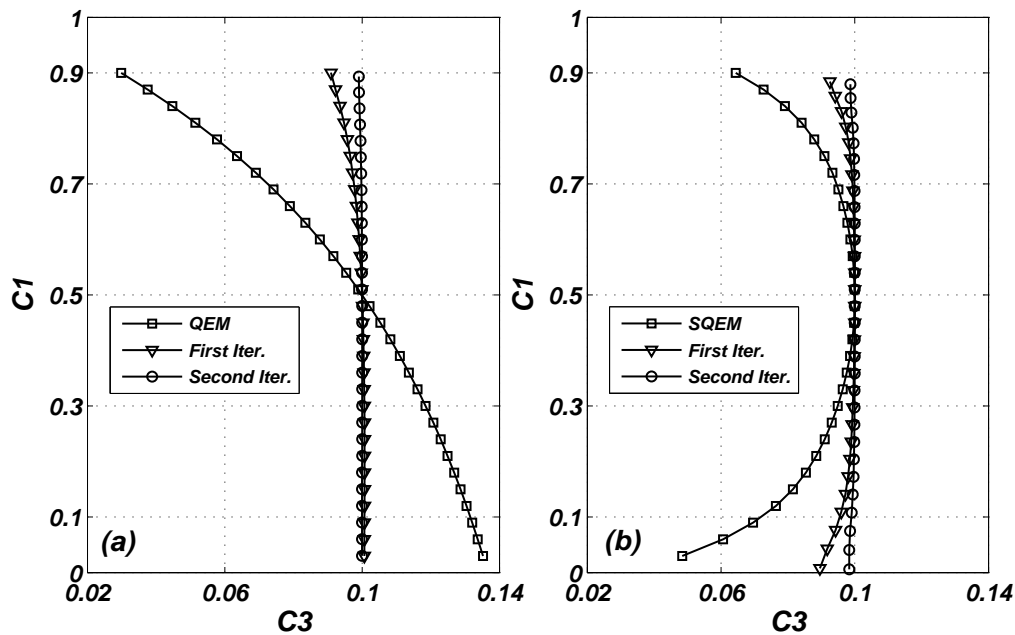


Figure 5: Newton method with incomplete linearization: (a) Two iterations starting from the QEM approximation; (b) Two iterations starting from the SQEM approximation.

(z_1, z_2, z_3, z_4) a generic four-dimensional vector which must be projected onto it, we can write:

$$\begin{cases} e_y = \omega f, & \omega = \frac{1}{DG(f)}, \\ Pz = DG(z)e_y = (\nabla G, z)e_y, \end{cases} \quad (3.20)$$

so that the null space of P has the following equation:

$$(\nabla G, z) = g_1 z_1 + g_2 z_2 + g_3 z_3 + g_4 z_4 = 0, \quad (3.21)$$

where $\nabla G = (g_1, g_2, g_3, g_4)$. The dimension of $S = (\ker P \cap \ker D)$ is 1; let b_1 be a vector which spans S .

When a set of concentration points is available (initial approximation of SIM), in each point c_0 , the Newton method must provide a correction ($c = c_0 + \delta c : \delta c = \delta_1 b_1$). Here, Eq. (2.26) takes the simple form:

$$\delta_1 = - \frac{((1-P)J, b_1)}{((1-P)Lb_1, b_1)}. \quad (3.22)$$

Figs. 5(a) and (b) show two initial grids taken on the QEM and SQEM respectively, composed by 30 grid-nodes, whose positions are refined by evaluating the (3.22) in each point. Results after the first and the second iteration are reported. Those initial grids

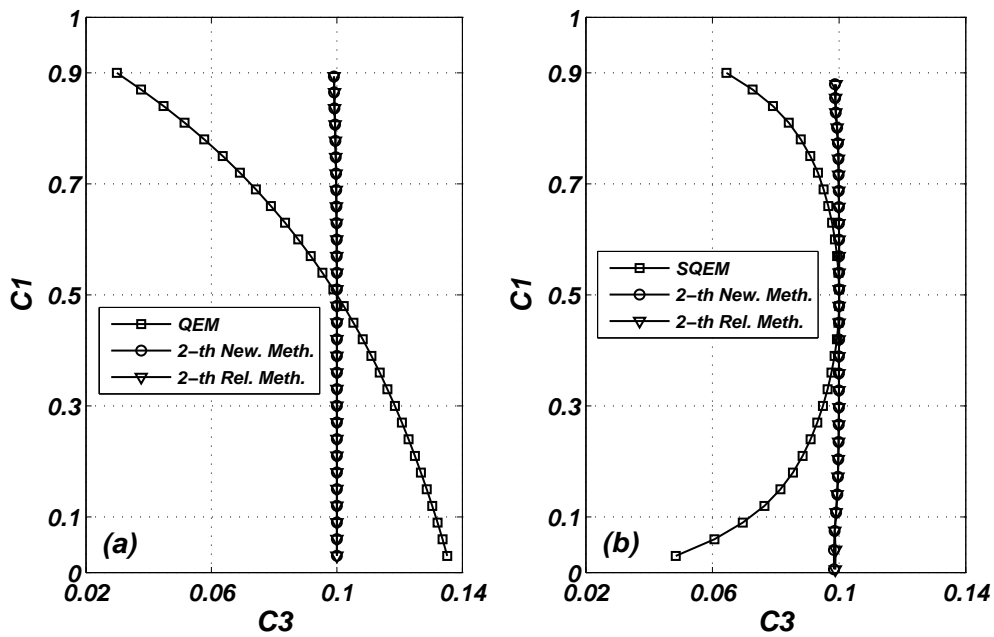


Figure 6: Comparison between Newton method and relaxation method: (a) Two iterations starting from the QEM approximation; (b) Two iterations starting from the SQEM approximation.

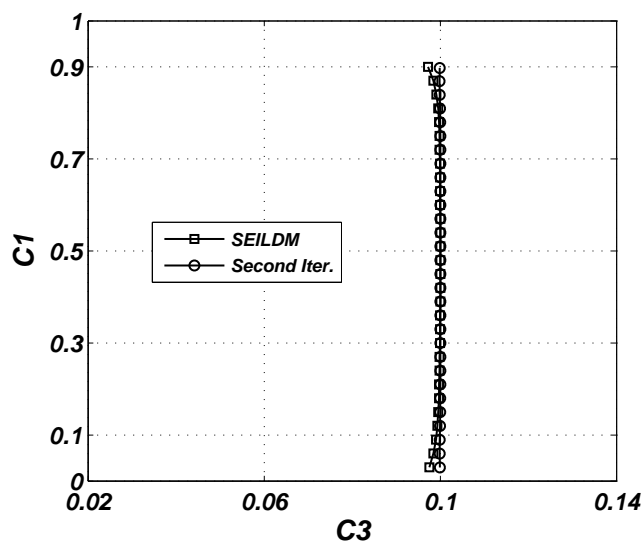


Figure 7: Newton method with incomplete linearization: Two iterations starting from the SEILDm approximation.

were also refined by the relaxation method using the projector (3.20) to calculate the invariance defect: in this case, formula (2.29) allows to compute the grid nodes correction.

In general, the relaxation method is expected to require a higher number of iterations than the Newton method to achieve a result of comparable accuracy. Nevertheless, this time because of the dimensionality of the problem the efficiency, as shown by Fig. 6, is very similar. Two Newton iterations were also performed starting from 30 nodes on the SEILD approximation (see Fig. 7).

3.5 Convergence of the invariance grid construction

Now it is instructive to compare the efficiency of the methods described above, by introducing some procedures able to estimate how the refined grid, in each iteration, is distant from the invariant one. That aim was reached utilizing two procedures. The first is based on the normalized Hausdorff distance (see also [6]) between two points sets, while the second one on the Euclidean norm of the invariance defect vector. In particular, let \hat{X}, \hat{Y} be the current set of grid points and the refined one on the SIM, if $d(x, y)$ denotes the standard Euclidean metric between two points, by definition the Hausdorff distance between \hat{X} and \hat{Y} is:

$$\delta_H = \frac{d_H}{D_H} 100\%, \quad (3.23)$$

where

$$\begin{cases} d_H = \max \left\{ \max_{x \in \hat{X}} \min_{y \in \hat{Y}} d(x, y), \max_{y \in \hat{Y}} \min_{x \in \hat{X}} d(x, y) \right\} \\ D_H = \max_{x, y \in \hat{X} \cup \hat{Y}} d(x, y). \end{cases} \quad (3.24)$$

Another way to evaluate the quality of an invariant grid approximation can be obtained considering the Euclidean norm of that vector which collects, in each grid point, the following measure of the invariance defect: $\sqrt{(\Delta, \Delta) / (J, J)}$. In the continuation, that value will be referred as to *Error*. The comparison between the two Figs. 8(a) and (b) shows that both those methods give compatible results. Here, we want to stress that if two initial grids are chosen, the most far one from the invariant manifold (e.g. in terms of Hausdorff distance) can also present a faster convergence (see QEM vs SQEM in Fig. 8). However, in general a closer initial grid to the invariant manifold gives better guarantees for the convergence of equations (2.26)-(2.29).

It is worth to note that all the grids found above (first approximation and refined ones) respect the thermodynamic requirement: indeed if they are traced from any point toward the equilibrium, the entropy ($-G$) increases (Fig. 9), thereby confirming the thermodynamic consistency of projector (3.20). Fig. 9 also provides the geometrical interpretation of a quasi equilibrium manifold: the tangent spaces to entropy curves in intersection points with the QEM have constant inclination.

3.6 CSP refinements

Also the refinement algorithms (2.33)-(2.34) were used to extract the SIM. This time we need to choose a set of vectors as initial approximation ($\mathbf{B}^{f,s}(0,0)$ and $\mathbf{A}_{f,s}(0,0)$ matrices).

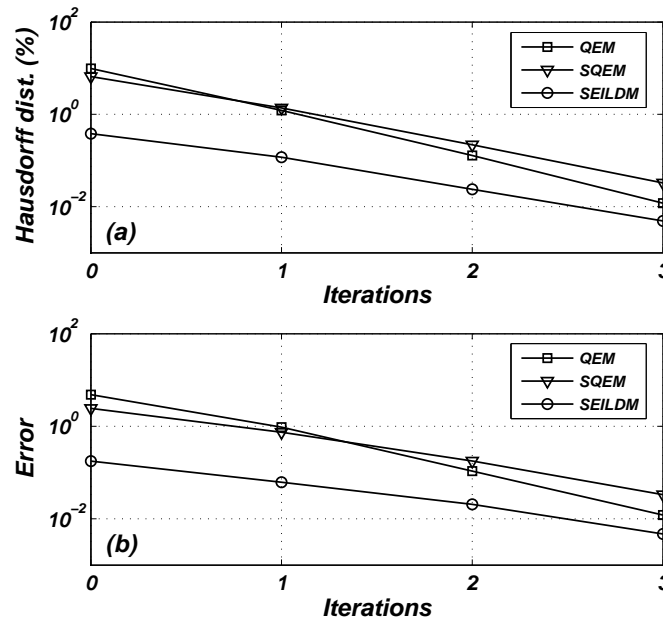


Figure 8: Newton method: (a) Hausdorff distance between refined grid and the invariant one; (b) Refined grid Error.

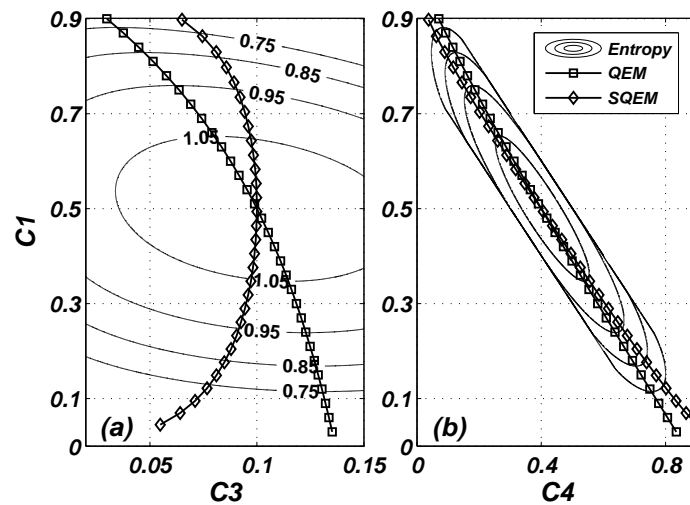


Figure 9: Entropy (-G) level curves: (a) QEM and SQEM in c_3-c_1 plane; (b) QEM and SQEM in c_4-c_1 plane.

For the system (3.13), the following vectors were chosen at the step ($k=0, m=0$):

$$A_f(0,0) = \left(\frac{\sqrt{2}}{2}, \frac{\sqrt{2}}{2}\right)^T, \quad A_s(0,0) = \left(-\frac{\sqrt{2}}{2}, \frac{\sqrt{2}}{2}\right)^T, \quad (3.25)$$

$$B^f(0,0) = \left(\frac{\sqrt{2}}{2}, \frac{\sqrt{2}}{2}\right), \quad B^s(0,0) = \left(-\frac{\sqrt{2}}{2}, \frac{\sqrt{2}}{2}\right). \quad (3.26)$$

It proves convenient to introduce functions

$$\begin{aligned} u &= -3c_3^2 + 0.9c_3 - 4c_3c_1 + 1.5c_1 - c_1^2 + 0.54, \\ v &= 5c_3^2 - 7.3c_3 + 3c_3c_1 - 2.3c_1 + 3.3, \\ w &= 6c_3^2 - 9.9c_3 + 2c_3c_1 - 2.1c_1 + 3.78, \\ \mu &= 1.7c_3^2 - 2.62c_3 + 1.7c_3c_1 - 0.16c_1 + 0.24, \\ \theta &= 3c_3 + c_1 - 1.8. \end{aligned}$$

Then the \mathbf{B}^f - \mathbf{A}_f -refinements can be written (see (2.33)-(2.34)):

$$\mathbf{A}_f(1,1) = \frac{1}{\sqrt{2}} \left(\frac{w}{v}, -\frac{u}{v} \right)^T, \quad \mathbf{A}_s(1,1) = \sqrt{2} \left(\frac{0.2 - c_3}{\theta}, \frac{2c_3 + c_1 - 1.6}{\theta} \right)^T, \quad (3.27a)$$

$$\mathbf{B}^f(1,1) = \sqrt{2} \left(\frac{2c_3 + c_1 - 1.6}{\theta}, \frac{c_3 - 0.2}{\theta} \right), \quad \mathbf{B}^s(1,1) = \frac{1}{\sqrt{2}} \left(\frac{u}{v}, \frac{w}{v} \right), \quad (3.27b)$$

$$\dot{\mathbf{B}}^f(0,0) = \dot{\mathbf{A}}_f(0,0) = \dot{\mathbf{A}}_f(1,0) = \mathbf{0}, \quad \dot{\mathbf{B}}^f(1,0) = \dot{\mathbf{B}}^f(1,1) = \sqrt{2} \left(\frac{\mu}{\theta^2}, -\frac{\mu}{\theta^2} \right). \quad (3.27c)$$

The approximate SIM is found from Eq. (2.35) which takes, at the step (1,0), the form:

$$2c_3^3 - 5.3c_3^2 + 2c_3^2c_1 - 2.5c_3c_1 + 3.66c_3 + 0.24c_1 - 0.32 = 0. \quad (3.28)$$

Eq. (3.28) provides three solutions and Fig. 10 reports only the relevant root (only one root is positive and real, and respects the balance condition (2.13)). Moreover, the manifolds related to the vectors $\mathbf{B}^f(0,0)$ and $\mathbf{B}^f(2,1)$ are also shown. Regarding to the latter manifold, we want to stress that now Eq. (2.35) gives one physically acceptable root among seven possible. Here the initial approximation coincides with the QEM, so it can be useful to compare MIG results with CSP ones on the base of Error (see Fig. 11). The derivatives (3.27c) show that the CSP procedure can become computationally intensive in few iterations even for a very simple example. Finally it is worth to comment Fig. 11(b): since every \mathbf{A}_f iteration does not increase the accuracy of \mathbf{B}^f vectors, the manifold, after the step (1,1), remains not refined.

4 Conclusion

In this paper, the method of invariant grids is utilized for reducing the kinetics of a simple two-dimensional system in order to obtain an one-dimensional description. Different initial approximations have been calculated and refined. It has been shown that the rate of convergence depends also, but not only, on the quality (distance from the invariant manifold) of initial approximation. Moreover, the SQEM is a convenient (for convergence) way to get the first grid: particularly when it is extended not far from the equilibrium point. In general, we found that the QEM construction is a very promising procedure to choose the initial manifold, and its efficient implementation in large dimension will

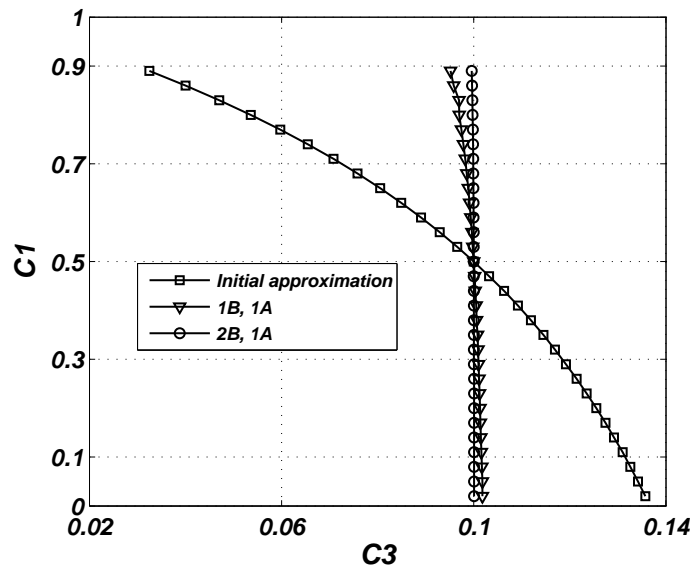


Figure 10: CSP refinement procedure.

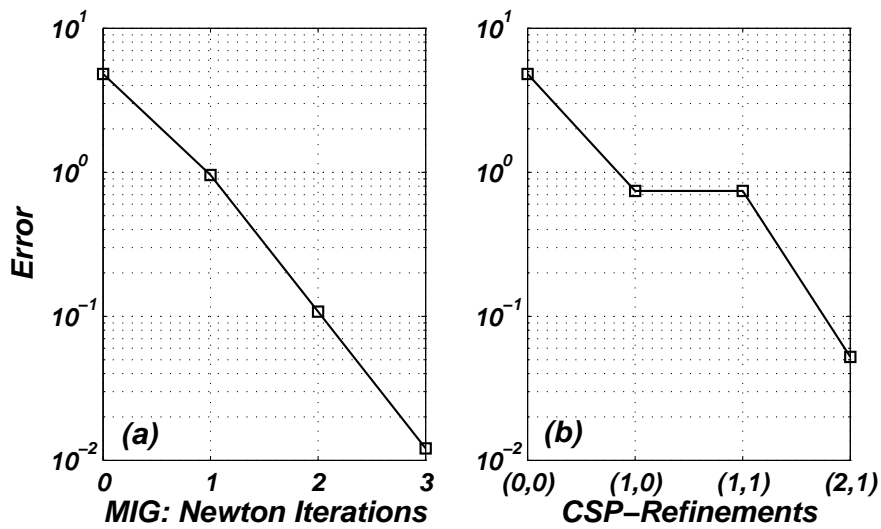


Figure 11: Error evolution during the iterations for (a) MIG and (b) CSP methods starting from the QEM approximation.

be presented elsewhere. As expected, the SEILDm approximation provides a manifold very close to the SIM without facing the full Jacobian matrix (ILDm), but just considering its symmetrized part. It was shown that the Newton method and the relaxation method give, when a 1D invariant grid is searched, comparable results. Nevertheless, in a general case, the Newton method is expected to be much more efficient, whereas the relaxation

method requires a lesser computational load. Therefore, it is worth to think of some hybrid procedures in which the Newton method and the relaxation method are used on different stages of computation. The CSP algorithm is utilized too and, although that method and MIG are based on completely different approaches, the comparison shows very similar results in terms of accuracy of SIM description.

The examples and computational approaches presented in this paper are implicitly based on a hypothesis about connected slow invariant manifold of fixed dimension. Nevertheless, we know that this hypothesis is not always true. In concentration space could exist areas with different dynamic behavior and different fast-slow separation. There is an important difference between areas where some of reactions go to their equilibrium faster than other do and areas where some of concentrations remain relatively small during long time. In the first case (fast equilibria), the slow motion goes near QEM, in second case (small concentrations), the quasi steady state (QSS) approximation could be used. Differences between smallness parameters and dynamical properties of QE and QSS were discussed, for example, in Refs. [2, 5]. In the quasi-equilibrium approximation for closed systems, both fast and slow motions inherit thermodynamic properties of the whole system and have simple dynamics with relaxation to equilibrium. Fast motion for QSS approximation can have bifurcation even if the whole system is isolated. These bifurcations are considered as models of critical effects, such as ignition (see, for example, Ref. [27]).

Already these two different situations with two types of small parameter could generate a complicated structure of approximate slow invariant manifolds and fast-slow separation in concentration space that is far from the picture presented on Fig. 1.

The choice of initial approximation and of the projector field could be also specifically discussed. CSP methods pretend to find optimal projector (fast directions) and SIM, both, but efficacy of this computations depends on initial approximation (i.e. on coordinate system). If we do not correct the projector field in computations, its pre-selection is even more important. For systems with separation of reversible reactions onto fast and slow, the reasonable initial approximation for slow manifold is QEM and its various modifications. The choice of projector in this case is also clear, the thermodynamic projector will work. The same is true near equilibrium, even if there is no obvious separation of reactions onto fast and slow. If we would like to continue these manifolds further from equilibrium, that choice could also give an appropriate result. But near a boundary of positivity the thermodynamic projector has singularity because of logarithmic singularity of chemical potentials near zero concentrations. In that case other projectors and scales could be used. Nevertheless, the notion of invariant grid and the sequence of construction: choice of projector field – invariance equation – iterative procedure remain universal.

Finally, in this paper we focused on the geometry of the model reduction, that is, construction of slow invariant manifolds (grids). Dynamic equations of the reduced system using the grid approach will be studied in a separate publication.

Acknowledgments

D. A. Goussis is gratefully acknowledged for the useful discussions about the CSP method. We thank K. B. Boulouchos, C. E. Frouzakis, I. Goldfarb and A. Yu. Zinovyev for discussions and suggestions. This work was partially supported by SNF, Project 200021-107885/1 (E.C.) and by BFE, Project 100862 (I.V.K.).

References

- [1] A. N. Gorban and I. V. Karlin, Thermodynamic parametrization, *Physica A*, 190 (1992), 393-404.
- [2] A. N. Gorban and I. V. Karlin, Method of invariant manifold for chemical kinetics, *Chem. Eng. Sci.*, 58 (2003), 4751-4768.
- [3] A. N. Gorban, I. V. Karlin and A. Y. Zinovyev, Invariant grids for reaction kinetics, *Physica A*, 333 (2004), 106-154.
- [4] A. N. Gorban, I. V. Karlin and A. Y. Zinovyev, Constructive methods of invariant manifolds for kinetic problems, *Phys. Rep.*, 396 (2004), 197-403.
- [5] A. N. Gorban and I. V. Karlin, Invariant manifolds for physical and chemical kinetics, *Lect. Notes Phys.* 660, Springer Berlin Heidelberg, 2005, DOI 10.1007/b98103.
- [6] A. N. Gorban, I. V. Karlin, V. B. Zmievskii and T. F. Nonnenmacher, Relaxational trajectories: Global approximations, *Physica A*, 231 (1996), 648-672.
- [7] R. Courant, K. O. Friedrichs and H. Lewy, On the partial difference equations of mathematical physics, *IBM J.*, 11(2) (1967), 215-234.
- [8] U. Maas and S. B. Pope, Simplifying chemical kinetics: Intrinsic low-dimensional manifolds in composition space, *Combust. Flame*, 88 (1992), 239-264.
- [9] V. Bykov, I. Goldfarb, V. Gol'dshtein and U. Maas, On a modified version of ILDM approach: Asymptotic analysis based on integral manifolds, *IMA J. Appl. Math.*, 71(3) (2006), 359-382.
- [10] S. H. Lam and D. A. Goussis, Conventional asymptotic and computational singular perturbation for symplified kinetics modelling , in: M. O. Smooke (Ed.), *Reduced Kinetic Mechanisms and Asymptotic Approximations for Methane-Air Flames*, Springer Lecture Notes, Springer, Berlin, 1991, pp. 227-242.
- [11] S. H. Lam and D. A. Goussis, The CSP method for simplifying kinetics, *Int. J. Chem. Kinet.*, 26 (1994), 461-486.
- [12] D. A. Goussis and M. Valorani, An efficient iterative algorithm for the approximation of the fast and slow dynamics of stiff systems, *J. Comput. Phys.*, 214 (2006), 316-346.
- [13] A. M. Lyapunov, *The General Problem of the Stability of Motion*, Taylor & Francis, London, 1992.
- [14] N. Kazantzis, Singular PDEs and the problem of finding invariant manifolds for nonlinear dynamical systems, *Phys. Lett. A*, 272 (2000), 257-263.
- [15] C. Foias, G. R. Sell and E. S. Titi, Exponential tracking and the approximation of inertial manifolds for dissipative nonlinear equations, *J. Dyn. Diff. Eq.*, 1 (1989), 199-244.
- [16] P. Constantin, C. Foias, B. Nicolaenko and R. Temam, Integral manifolds and inertial manifolds for dissipative partial differential equations, in: *Applied Math. Sci.*, vol. 70, Springer Verlag, New York, 1988.
- [17] J. C. Robinson, A concise proof of the "geometric" construction of inertial manifolds, *Phys. Lett. A*, 200 (1995), 415-417.

- [18] A. Debussche and R. Temam, Inertial manifolds and slow manifolds, *Appl. Math. Lett.*, 4 (1991), 73-76.
- [19] L. B. Ryashko and E. E. Shnol, On exponentially attracting invariant manifolds of ODEs, *Nonlinearity*, 16 (2003), 147-160.
- [20] R. S. MacKay, Slow manifolds, in: T. Dauxois, A. Litvak-Hinenzon, R. S. MacKay and A. Spanoudaki (Eds.), *Energy Localisation and Transfer*, World Sci., 2004, pp. 149-192.
- [21] A. N. Gorban and I. V. Karlin, Uniqueness of thermodynamic projector and kinetic basis of molecular individualism, *Physica A*, 336 (2004), 391-432.
- [22] H. G. Kaper and T. J. Kaper, Asymptotic analysis of two reduction methods for systems of chemical reactions, *Physica D*, 165 (2002), 66-93.
- [23] N. Kazantzis, Singular PDEs and the problem of finding invariant manifolds for nonlinear dynamical systems, *Phys. Lett. A*, 272(4) (2000), 257-263.
- [24] M. R. Roussel and S. J. Fraser, On the geometry of transient relaxation, *J. Chem. Phys.*, 94 (1991), 7106-7113.
- [25] M. R. Roussel and S. J. Fraser, Geometry of the steady-state approximation: Perturbation and accelerated convergence methods, *J. Chem. Phys.*, 93 (1990), 1072-1081.
- [26] S. J. Fraser, The steady state and equilibrium approximations: A geometrical picture, *J. Chem. Phys.*, 88 (1988), 4732-4738.
- [27] J. N. Bradley, J. A. Barnard and J. F. Griffiths, *Flame and Combustion*, Blackie, London, 1995.